JOURNAL OF Materials CHEMISTRY

Zeolitization of diatomite to prepare hierarchical porous zeolite materials through a vapor-phase transport process

Yajun Wang, Yi Tang,* Angang Dong, Xingdong Wang, Nan Ren and Zi Gao

Laboratory of Molecular Catalysis and Innovative Materials, Department of Chemistry, Fudan University, Shanghai 200433, P. R. China. E-mail: ytang@fudan.ac.cn

Received 31st January 2002, Accepted 28th March 2002
First published as an Advance Article on the web 16th April 2002

In this study, we report a new, simple approach to the preparation of hierarchical structured zeolites through transforming the diatomaceous silica into zeolite by a vapor-phase transport (VPT) method. The morphology and macro-porosity of the diatomite are well preserved even in the samples with zeolite content higher than 50%. The products possess high mechanical strength and hydrothermal stability, and are thus promising for application in catalysis, adsorption and separation. The influence of the zeolite structures, the amount of adsorbed seeds, and the VPT treatment time and temperature on the crystallinity of the resulting materials are discussed. Powder XRD, SEM, TEM, IR and N_2 adsorption–desorption measurements are employed to monitor the VPT treatment process.

1 Introduction

It is known that zeolites are crystalline materials with wide use in shape-selective catalysis and molecular sieving separation because of their strong acidity, good thermal/hydrothermal stability and uniform channels in the microporous regime.[1] However, relatively slow mass transport through their small micropores (<1 nm) has been one of the main concerns, which greatly limit the utilization of the zeolites. Hierarchical structured zeolites, especially the macro–micro or meso–micro bimodal porous zeolite materials, are attracting considerable research enthusiasm for the purposes of creating shorter diffusion paths to improve the efficiency of catalysis and separation. General strategies for synthesizing such materials rely on the use of removable templates, which dictate the macroporous architecture of the final products.[2–14] For example, polystytrene (PS) beads were recently used as a second template in a dual template approach to obtain macro–micro porous materials with a semi-crystalline silicalite-1 framework.[2] Using a similar strategy, Jacobsen and co-workers employed mesoporous carbon blacks[3] or carbon nanotubes[4] as templates to prepare zeolites containing a mesoporous structure. Using the self-assembly properties of zeolite nanocrystals, the macro–micro porous zeolite materials have also been produced by the infiltration of silicalite-1 colloids into an ordered array of PS latex with subsequent calcination.[5,6] Rhodes *et al.*[7] and Wang *et al.*[8] independently employed the layer-by-layer (LbL) assembly technique to fabricate hollow zeolite spheres through PS beads templating nearly at the same time. Ke *et al.*[9] reported an electrophoretic deposition technique to assemble zeolite nanocrystals on carbon fibers, and the zeolite hollow fibers were obtained upon calcination. However, in all these strategies, a great amount of organic templates must be removed by calcination or extraction to obtain the porous structure. More importantly, the inferior mechanical strength of the macroporous materials after the removal of the templates greatly limited their practical applications.

To overcome these disadvantages, an alternative route to prepare multi-level porous materials with higher thermal and mechanical stability is to use stable templates with intrinsic hierarchical structures. Diatomite is one of the perfect candidates for its inherent macroporous structure, inexpensiveness and easy availability. Owing to its favorable properties, diatomite has been widely used as filters, abrasives and sound and heat insulators. Recently, Anderson and co-workers[15,16] have zeolitized the diatomite through hydrothermal treatment of the ultrasonic seeded or un-seeded diatomite in clear synthesis solutions containing adscititious silicon or aluminium sources. However the characteristic array of submicron pores, and even the larger internal voids of the barrel-like diatomite, were blocked by the overgrown zeolite crystals during the zeolitization process, leading to a decrease of the diffusion channels. To maintain the intact diatomaceous submicron pore arrays, we previously adopted a LbL assembly strategy to zeolitilize diatomite.[17] Although this method is easier to control both the thickness and composition of the zeolite coatings on diatomite substrate, it seems not to be appropriate for practical applications due to the low zeolite content in the final samples.

This paper is attempting to find a more economical and facile method to effectively zeolitilize the diatomaceous silica while still keeping the original macroporous structure of the diatomite. Herein, the vapor phase transport (VPT) process, a method which has been widely used to prepare zeolites from the artificial dry-gel with pre-designed composition and morphology,[18–20] was successfully extended to the transformation of the diatomaceous silica into zeolite in the aid of the nanozeolite seeds. The macro-porosity of the diatomite is well preserved even in the samples with zeolite content higher than 50%. The roles of the seeds, and the VPT treatment time and temperature are discussed. The products were characterized by powder X-ray diffraction (XRD), scanning electron microscopy (SEM), transmission electron microscopy (TEM), energy diffraction spectra (EDS), Infrared (IR), Thermogravimetric analysis (TGA) and N_2 adsorption–desorption measurements.

2 Experimental

2.1 Reagents

Tetraethoxysilane (TEOS, 98%), tetrapropylammonium hydroxide (TPAOH, 1 M), and polyelectrolyte poly(diallyldimethylammonium chloride) (PDDA, $M_w < 200\,000$) were obtained from Aldrich. Aerosil 400 (99.8 wt%, Shanghai electrochemical factory), tetraethylammonium hydroxide (TEAOH, 25 wt% in water, $Na^+ < 10$ ppm $< K^+ < 5$ ppm, Shanghai reagent company), and aluminium foils (99.5%, Shanghai reagent

 DOI: 10.1039/b201113a

This journal is © The Royal Society of Chemistry 2002

company) were used as received. The diatomite was obtained from Changbai Diatomite Ltd, Jilin Province of China with listed components of SiO_2 86.7%, Al_2O_3 4.5%, Fe_2O_3 1.23%, CaO 0.44%, MgO 0.43%, TiO_2 0.4%, K_2O + Na_2O *ca.* 0.9–1.1%, and purified with a sedimentary method in distilled water to remove the mixed scrappy minerals before use.

2.2 Preparation of seed colloids

The suspension of nanosized silicalite-1 crystals with an average size of 80 nm were synthesized from a clear mixture with the molar composition $9\,TPAOH : 25\,SiO_2 : 480\,H_2O : 100\,EtOH$ according to the procedure described in ref. 21. The starting materials were TEOS, TPAOH, and distilled water. After pre-hydrolysis of the solution on a shaker at room temperature for 24 h, it was subjected to hydrothermal treatment at 100 °C for 48 h. The synthesis of colloidal β zeolite (45 ± 5 nm) seeds was carried out in a basic medium without alkali cations as described in the literature.[22] Typically, 0.100 g aluminium foil was first dissolved in TEAOH. This solution was then added to a mixture made by dispersing aerosil in a solution of TEAOH under vigorous stirring. The final reaction mixture has the molar composition of $15\,TEAOH : 30\,SiO_2 : 1\,Al_2O_3 : 480\,H_2O$, which was aged for 2 days at room temperature and then subjected to hydrothermal synthesis at 140 °C for 14 days in a sealed stainless steel autoclave lined with poly(tetrafluoroethylene).

The nanosized crystals resulting from hydrothermal treatment were purified through four-steps of centrifugation (15 000 rpm, 30 min). After each step of centrifugation, the nanoparticles were redispersed in distilled water by using an ultrasonic bath for 20 min, while after the fourth centrifugation step the nanoparticles were resuspended in distilled water with a concentration of approximately 0.5 wt% (pH 9.5, adjusted with 0.1 M ammonia solution).

2.3 Diatomite seeding process

The diatomite seeding process was fulfilled by a method previously described in the literature.[17] First, the diatomite was modified with one layer of cationic PDDA. Then, the nanozeolites and PDDA were alternately deposited on the pre-modified diatomite substrates with desired PDDA/nanozeolite deposition cycles to form homogeneous zeolite/PDDA multilayers. All the adsorption steps were done in a deposition suspension with a liquid : solid volume ratio of 50 for a duration of 20 min, followed by rinsing with 0.1 mol L^{-1} NH_4OH solution for four times to remove the excess nanozeolites or polyelectrolyte. The initial diatomite and the diatomite seeded through different cycles are denoted as DS-*m* ('*m*' indicates the number of deposition cycles).

2.4 VPT treatment process

Typically, 0.2 g of nanozeolite seeded diatomite was dispersed on a porous stainless steel board, which was placed horizontally in the middle of a stainless steel autoclave and 2 g of a liquid mixture of ethylenediamine, triethylamine and H_2O with the molar ratio of 2 : 9 : 6 was injected into the bottom of the autoclave. Then the autoclave was sealed and placed in an oven at the desired temperature for several days. In a similar manner, the DS-*m* samples after VPT treatment are denoted as DS-*m*(*n*) ('*n*' indicates the VPT treatment time in days). After the VPT treatment, the samples were heated up to 550 °C from room temperature at a heating rate of 5 K min^{-1}, and kept for 8 h in flowing air.

2.5 Characterization

Powder X-ray diffraction (XRD) was carried out with a Rigaku D/MAX-IIA instrument using Cu Kα radiation at 35 kV and 20mA. The average crystal sizes of the samples are calculated from the broad XRD lines of the (011) and (200) reflections using the Scherrer equation, and KBr powder was employed as an internal reference. Morphologies were examined by micrographs obtained through scanning electron microscopy (SEM, Philips XL30). High-resolution transmission electron microscope (HRTEM) images and energy diffraction spectra (EDS) data were obtained on a JEOL JEM-2010 transmission electron microscope. Infrared (IR) spectra were recorded on a Magna 550 spectrophotometer using KBr pellets. Thermogravimetric analysis (TGA) was performed on a Rigaku thermogravimetric analyzer. The samples were heated under flowing air from 25 to 800 °C at 5 K min^{-1}. N_2 adsorption–desorption measurements were conducted on a Micromeritics ASAP 2000 apparatus at 77 K using nitrogen as the adsorption gas.

3 Results and discussion

3.1 Characterization of the original diatomite

To study the morphology and architecture of the initial diatomite substrates, scanning electron microscopy (SEM) and powder X-ray diffraction (XRD) were applied. Fig. 1 shows the SEM images of the initial diatomite at different magnifications. The initial diatomite shows a disc-like shape with a thickness of *ca.* 1.2 μm and diameter of *ca.* 20–40 μm (Fig. 1a). There is a nearly regular array of submicron pores in a diameter range of 300–500 nm on the disc, and the surface of the diatomite disc seems very smooth when it is observed at a high magnification (Fig. 1b). The pore size near the center of the diatomite disc is larger but smaller near the disc edge. To compare the morphology changes during the zeolitization process, the SEM images in the following contents are taken on the center range of the diatomite disc. The initial diatomite has an XRD pattern

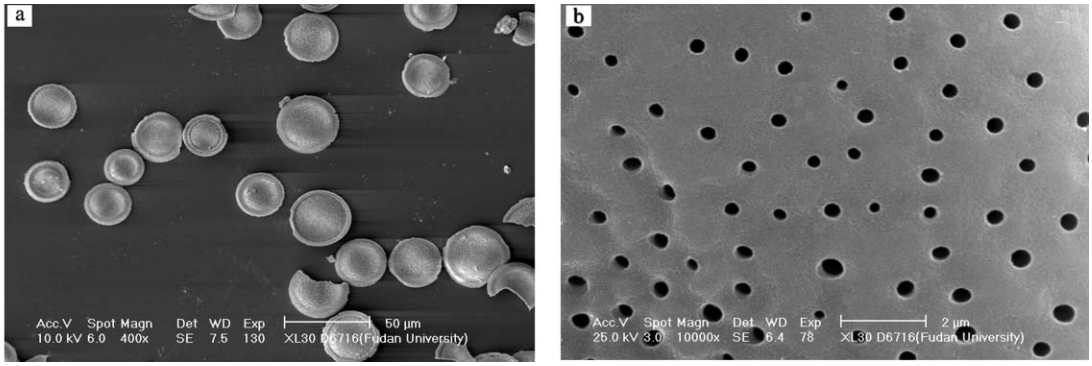

Fig. 1 SEM images of the initial diatomite at low (a) and high (b) magnifications.

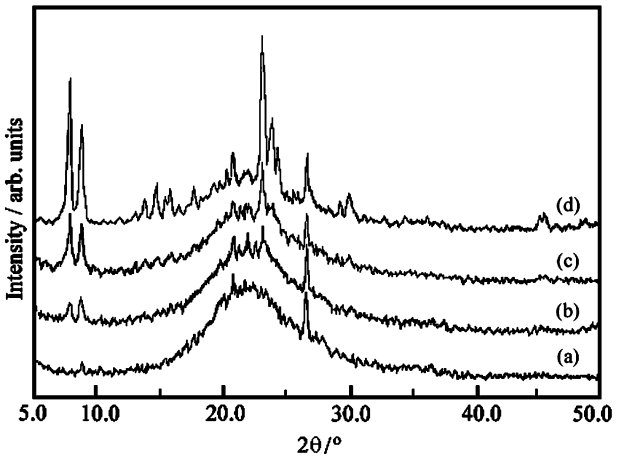

Fig. 2 XRD patterns of the initial diatomite (a), diatomite seeded through one (b) and three (c) PDDA/nanosilicalite-1 deposition cycles, and VPT treatment of sample (b) for five days (d).

mainly consistent with amorphous silica and a small amount of quartz and cristobalite (Fig. 2a). Approximately 85% of the diatomite is amorphous SiO_2 and 4.5% is Al_2O_3, hence it is possible to prepare the zeolite only by utilizing the diatomite as silica and aluminium sources.

3.2 Effect of the seeds

We have tried to transform the amorphous diatomaceous silica directly into zeolite through treating the unseeded diatomite under a mixed vapor of volatile amine and steam. However, no zeolite phase is detected in the XRD pattern after VPT treatment except the slight dissolution of the diatomite. It seems that the diatomaceous silica is not active enough to be directly transformed into zeolite only by contact with vapors of water and volatile amines. Hence, the colloidal zeolite seeds are adopted to induce the zeolitization of the diatomite. The seeding process is fulfilled through a layer-by-layer (LbL) electrostatic deposition method, which has been widely applied to assemble nanosized 'building blocks' previously.[7,8,23–26] The SEM image (Fig. 3a) shows that the diatomite surface is completely and homogeneously covered with a layer of silicalite-1 nanocrystals after only one electrostatic deposition cycle.

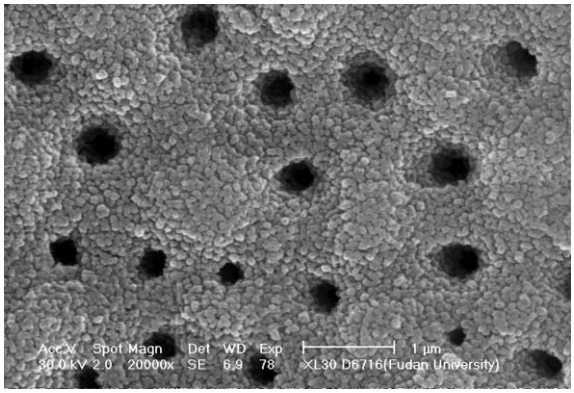

Fig. 4 SEM image of the DS-1(5) sample.

After treating the seeded diatomite (DS-1) samples under a mixed vapor of ethylenediamine, triethylamine and water at 180 °C for five days [denoted as DS-1(5)], the intensity of the characteristic MFI-structured zeolite peaks obviously increases (Fig. 2d), indicating the increase of the sample crystallinity. No other crystalline phases are found to occur in the treated samples compared with the initial diatomite. From the N_2 sorption data listed in Table 1, it could be found that the micropore surface area of the DS-1(5) sample is much higher than the untreated DS-1 sample, implying the increase of zeolite content in VPT treated samples.

Fig. 4 shows the SEM image of the DS-1(5) sample. After the VPT treatment, the disc morphology and hierarchical pore structure of the diatomite are both well preserved. The zeolite

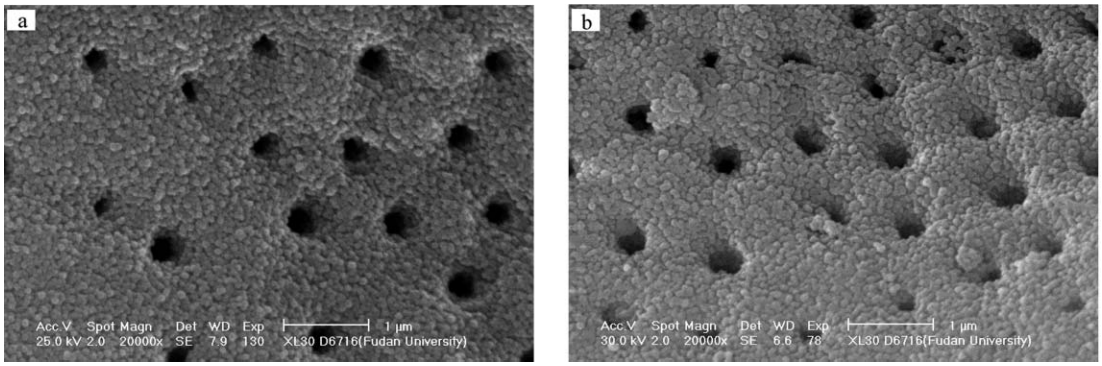

Fig. 3 SEM images of the DS-1 (a) and DS-3 (b) samples.

Table 1 N_2 adsorption–desorption results of the initial, silicalite-1 nanocrystal seeded, and VPT treated diatomite

Samples	S_{BET}/m^2 g^{-1}	$S_{Langmuir}$/m^2 g^{-1}	$S_{external}$[a]/m^2 g^{-1}	$V_{micropore}$[b]/cm^3 g^{-1}	$S_{micropore}$[a]/m^2 g^{-1}	$W_{zeolite}$[c](%)
DS-0	9	12	5	0.002	3	—
DS-0(5)	12	17	8	0.002	4	—
DS-1	26	34	9	0.009	16	4.7
DS-3	44	60	16	0.018	28	10.7
DS-1(5)	119	160	40	0.042	79	27.0
DS-2(5)	122	164	36	0.045	87	29.1
DS-3(5)	130	160	35	0.050	99	32.4
DS-1(10)	210	268	67	0.078	143	51.4
Silicalite-1 seeds	358	476	97	0.148	261	100

[a]Calculated from the Brunauer–Emmett–Teller (BET) surface area. [b]The volume of micropores, $V_{micropore}$, was determined by the *t*-plot method. [c]The weight% of zeolite in the final samples, $W_{zeolite}$%, was calculated from the micropore volume using the equation: $W_{zeolite}\% = \{V_{micropore}[\text{DS-}m(n)] - V_{micropore}(\text{DS-0})\} \times 100\%/V_{micropore}$ (silicalite-1 seeds).

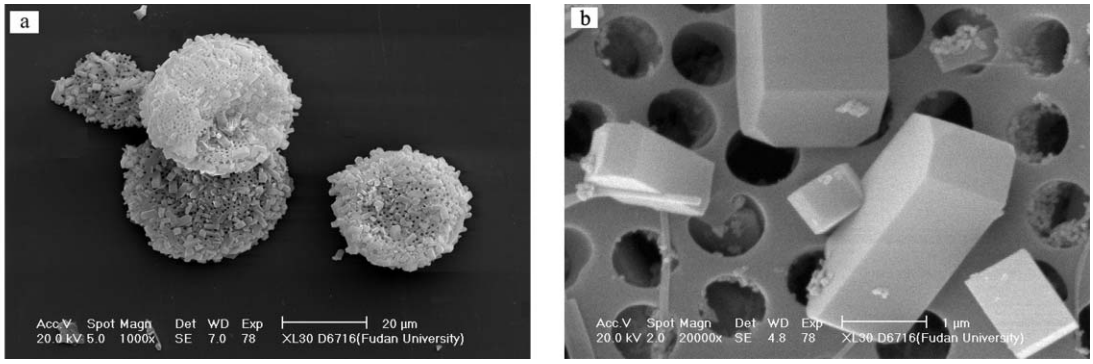

Fig. 5 SEM images of the VPT treated diatomite seeded with zeolite β nanocrystals at low (a) and high (b) magnifications.

crystals are homogeneously dispersed on the diatomite surface, and their crystal sizes are increased very slightly.

To investigate the influence of the seed layers and/or amount, multiple seed deposition cycles are applied. The multilayers of colloidal silicalite-1 coated diatomite substrate are prepared by repeating the sequence cationic polymer/silicalite-1 seed adsorption. With the deposition cycles increasing, the deposited zeolite amount is gradually increased, judged from the XRD (Fig. 2b,c) and N_2 adsorption–desorption data (Table 1). The diatomite morphology could be roughly kept within four deposition cycles, except that the pore size on the diatomite disc gradually reduces with the increasing number of deposition cycles (Fig. 3b).

After VPT treatment of the diatomite seeded with different amounts of silicalite-1 nanocrystals at 180 °C for five days, the surface areas of the multilayer silicalite-1 coated diatomite are only slightly larger than the monolayer seeded diatomite. The DS-1(5), DS-2(5) and DS-3(5) samples possess a surface area of 119, 122, and 130 $m^2\ g^{-1}$, respectively. Similar surface areas among the DS-1(5), DS-2(5) and DS-3(5) samples implies that the increase of the surface area in the samples is mainly attributed to the zeolitization of the diatomaceous silica, and a monolayer of seeds is sufficient to induce the zeolitization process.

Besides the MFI-structured zeolite, we even attempted to zeolitize the diatomaceous silica into other structured high silica zeolites, *e.g.* zeolite β, a three-dimensional large micropore zeolite with BEA topology structure.[27] In this case, one layer of zeolite β nanocrystals are seeded onto the diatomite substrates to induce such a transformation. Surprisingly, after VPT treatment with the same conditions, only larger crystals are found in the samples (Fig. 5a). At higher magnification (Fig. 5b), we could find that most of the crystals are tightly rooted in the diatomite plate and the pore diameter of the diatomite characteristic pore arrays is obviously widened when compared with the original diatomite (Fig. 1b). These phenomena clearly indicate that the large crystals are grown through consuming the diatomaceous silica source. However, XRD spectra show that these larger crystals are not zeolites with BEA structure, but with a well-crystallized MFI topology structure (Fig. 6). The transformation of the BEA to MFI structures might be caused by insufficient stability of nanosized zeolite β to survive the high temperature and alkalinity so that the MFI-structured zeolites are preferentially formed under these conditions. However, why only the discrete, larger zeolite crystals but not a continuous zeolite membrane are formed on the diatomite substrate is not quite clear.

3.3 Effect of the treatment conditions

Besides the inductive effect provided by the zeolite seeds, the temperature is another important factor which can influence the zeolitization degree of the diatomite. The effect of temperature on the zeolite content in the final products is depicted in Fig. 7. The crystallinity of the samples changes little after treatment below 140 °C for ten days. With an increasing of temperature, the amorphous diatomaceous silica begins to be transformed into zeolite effectively, and only the MFI-structured zeolite phase is detected at *ca.* 160–180 °C. However, when the temperature is further increased to about 200 °C, some unknown crystal phases are observed and the zeolite MFI content is slightly decreased.

The influence of the treatment time is also investigated at 180 °C. After 5 and 10 days of treatment, the obtained samples had BET surface areas of 120 and 210 $m^2\ g^{-1}$, respectively. With a further increase in the treatment time, no increase of the surface area is observed. About half of the diatomaceous silica

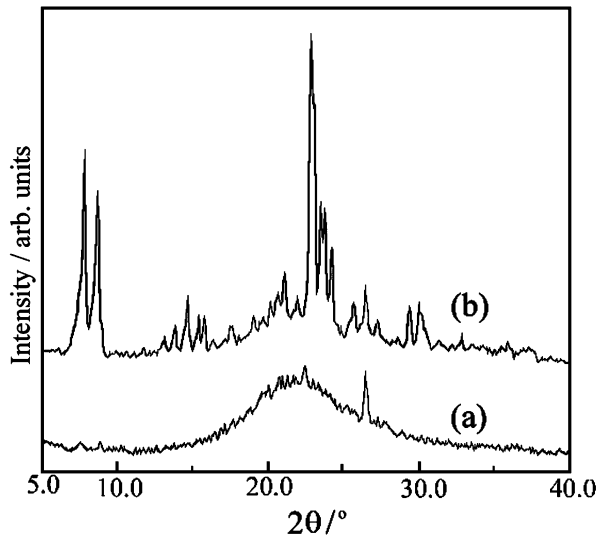

Fig. 6 XRD patterns of the diatomite seeded with one layer of zeolite β nanocrystals (a), and VPT treatment of sample (a) for five days (b).

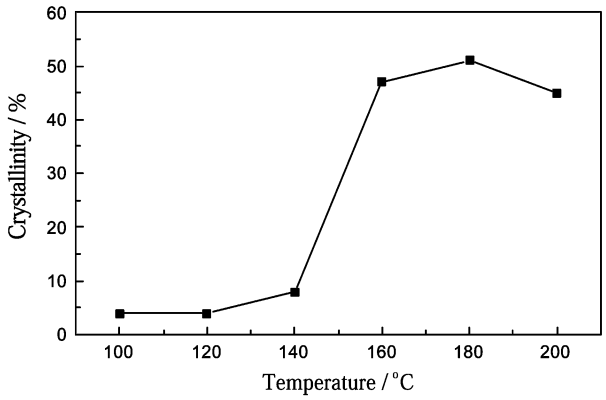

Fig. 7 Influence of the VPT treatment temperature on the zeolitization of diatomite.

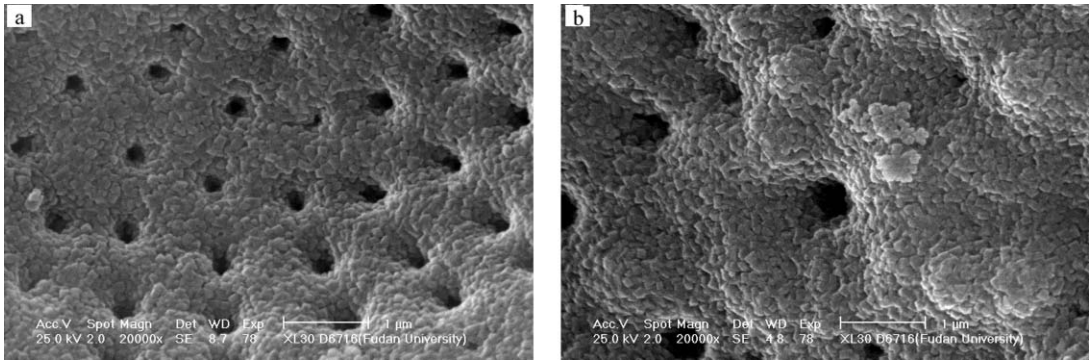

Fig. 8 SEM images of the DS-1(10) (a) and DS-1(20) (b) samples.

is converted into zeolite in the final samples (see Table 1). Fig. 8 shows the SEM images of the DS-1 samples treated after different periods. When the treatment time is longer than 5 days, the zeolite particles are more closely linked together and converted to quadrate crystals from the original spherical morphology, but the zeolite seed crystal size is only slightly increased even after 20 days of treatment. No zeolite crystals are found to grow apart from the diatomite plates in all SEM images. The well preserved hierarchical pore structure of the diatomite in our experiment might be explained by the fact that no additional silica or aluminium source is added into the initial reaction system and the migration of diatomaceous silica is also restrained during VPT treatment since the diatomite is separated from the alkaline solution, which largely restrains the diatomite dissolution and extraneous zeolite crystallization. Hence, the relatively mild and controllable VPT process might be more favorable to keep the diatomite hierarchical structures than the traditional hydrothermal process.[15,16]

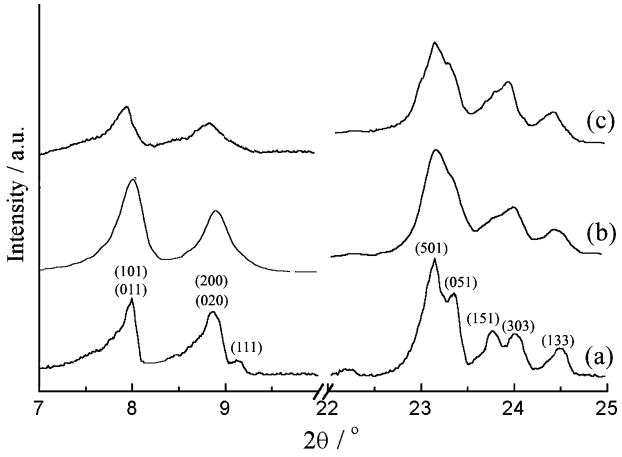

Fig. 9 XRD patterns of the silicalite-1 samples with crystal size of *ca.* 5 μm (a), 80 nm (b), and DS-1(10) sample (c).

3.4 Product characterization

Thermogravimetric analysis is carried out to survey the process of the removal of organic compounds (*e.g.* amines, PDDA, TPAOH, *etc.*) during the calcination. At $T < 170$ °C, there is a nearly identical weight loss (*ca.* 2%) in both DS-1 and DS-1(10) samples due to the desorption of water and adsorbed organic amine molecules. At $T > 170$ °C, the weight loss of the DS-1 and DS-1(10) samples are *ca.* 1.2 and 4.8%, respectively, owing to the decomposition of occluded organic molecules. The larger weight loss in the DS-1(10) sample shows that some ethylenediamine and/or triethylamine are occupied in the samples (most probably as the templates in the newly formed zeolite micropores) after VPT treatment. In both cases, the emission of waste gas from the decomposition of organic templates is much less than that of previous ways of obtaining the hierarchical structured zeolites templated by polystytrene beads,[2,5–8] carbon fiber[9,12,13] or other removable macropore templates.[3,4,10] Therefore, the utilization of natural diatomite to prepare hierarchical zeolites might provide an more economical and environmentally friendly process in which very small amounts of organic species are included in the samples.

After VPT treatment of the DS-1 samples for ten days, the intensity of the characteristic MFI-structured zeolite peaks greatly increases. However, the widths of the diffraction peaks change little compared with the original silicalite-1 nanocrystals, and are obviously broader than those of large silicalite-1 crystals (Fig. 9). The obvious widening of the diffraction peaks indicates that the materials are still comprised of nanosized zeolite crystals. The average crystal size of DS-1(10) is 70–120 nm, calculated by the XRD line broadening of the (011) and (200) reflections using the Scherrer equation.

Compared with the initial and silicalite-1 seeded diatomite, the IR spectrum (Fig. 10) of the DS-1(10) sample shows typical Si–O–Si framework bands including the characteristic double ring vibration at *ca.* 550 cm^{-1} in the MFI-structured zeolites,[28] indicating the increase of zeolite content in the products.

HRTEM further confirms the presence of nanocrystals in the size range of 80–140 nm with a quadrate morphology after VPT treatment (Fig. 11a). Lattice fringes are seen to extend throughout the entire crystal, demonstrating the high crystallinity of the nanocrystals (Fig. 11b). Energy diffraction spectra (EDS) analysis gives a component of $28\,SiO_2 : 0.45\,Al_2O_3 : 0.08\,Fe_2O_3 : 0.08\,K_2O : 0.07\,CaO$ in the zeolite nanocrystals.

The hydrothermal stability of the DS-1(10) is studied through hydrothermal treatment of the samples at 1073 K for 8 h under 100% steams, a process of simulated catalyst ageing in the commercial process with severe conditions to

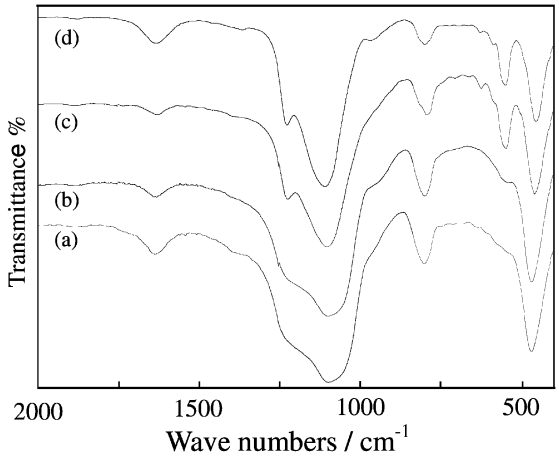

Fig. 10 IR spectra of the initial diatomite (a), DS-1 (b), DS-1(10) (c), and nanosized silicalite-1 (d) samples.

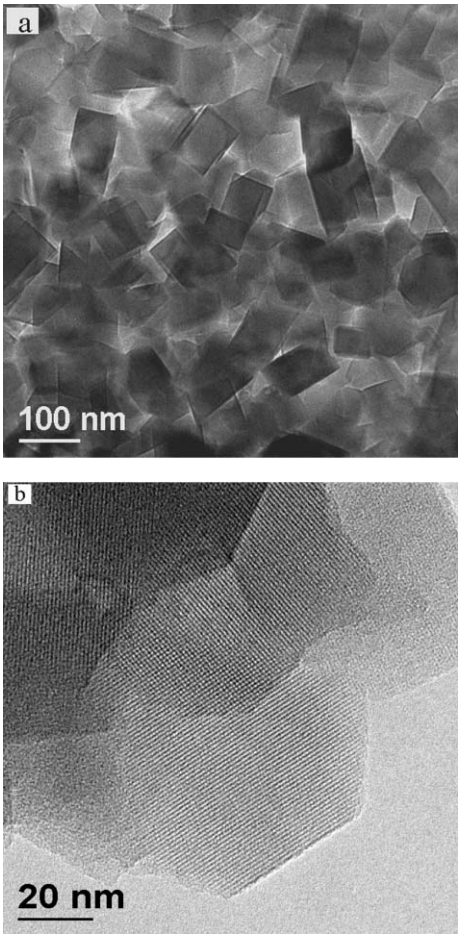

Fig. 11 HRTEM images of the calcined DS-1(10) sample at low (a) and high (b) magnifications.

research the hydrothermal deactivation of zeolites.[29] The characteristic peaks of MFI-structured zeolite are still well preserved in the XRD pattern (Fig. 12b), indicating that the zeolite crystals are very stable upon hydrothermal treatment at 1073 K. The mechanical stability of DS-1(10) is determined through sonication treatment. This process is carried on for 30 min using a sonic bath (HF frequency = 50 kHz, 120 W). No exfoliation of the zeolite particles is found in the samples. The SEM image shows that the zeolite nanocrystals are still

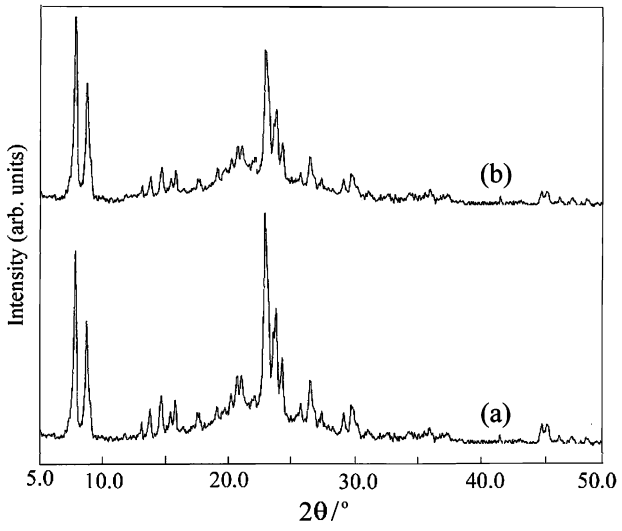

Fig. 12 XRD patterns of the DS-1(10) sample calcined at 550 °C (a), and after hydrothermal treatment at 800 °C under 100% steam for 8 h (b).

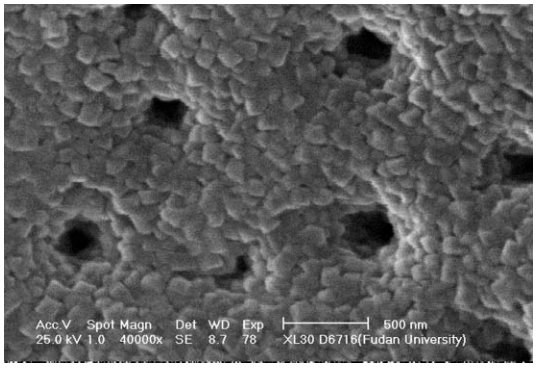

Fig. 13 SEM image of the calcined DS-1(10) sample after sonication treatment for 30 min.

tightly bound to the diatomite substrate after sonication treatment (Fig. 13).

The adsorption properties of the products are determined by the benzene adsorption experiment. The benzene adsorption amounts of DS-1(5) and DS-1(10) are 2.6 and 4.6%, respectively. The adsorption amount per unit area is 2.8 μmol m^{-2}, close to the value of ZSM-5 (2.7 μmol m^{-2}, supposing that the surface area is *ca.* 400 m^2 g^{-1} and the adsorption amount of benzene is 8.4%[30]). However, benzene is scarcely adsorbed on the initial diatomite. The benzene adsorption experiment also confirms the existence of well-crystallized zeolites in the samples. Although at most half of the diatomaceous silica could be transformed into zeolite by the present method, the products are expected to be efficiently utilized since the newly formed zeolite phase is mainly focused on the surface layers of the hierarchical structured diatomite substrates, which is very favorable for the transportation of guest species and the full utilization of zeolite micropores.

Conclusions

This study has demonstrated that the vapor-phase transport process is an effective method to zeolitize natural diatomite with the inducement of nanosized zeolite seeds. The zeolite structures of the seeds play a very important role in the transformation process, and a layer of seeds is sufficient to induce the zeolitization process. The ideal treatment temperature is between 160 and 180 °C in the ethylenediamine, triethylamine and H_2O system. With the increase of treatment time, the zeolite content was gradually increased within ten days and about half of the diatomaceous silica is converted into zeolites in the final samples. The hierarchical structure of the original diatomite is well preserved in all of the samples prepared from silicalite-1 colloid seeded diatomite. The HRTEM and benzene adsorption experiments prove the existence of well-crystallized zeolite in the samples. Furthermore, the products are thermally stable, and have good mechanical and hydrothermal stability, which would meet the practical applications in catalysis, adsorption, and separation. In addition, the described approach is also an economical and environmentally friendly process in which the need to remove a great amount of organic species is eliminated. This process may also be extended to zeolitize other silica-containing natural substrates in principle.

Acknowledgements

This work is supported by the Major State Basic Research Development Program (Grant No. 2000077500), the NNSFC (Grant No. 29873011), the Foundation for University Key Teacher by the Ministry of Education and the Doctoral Fund of Chinese Education Ministry.

References

1 M. E. Davis, *Ind. Eng. Chem. Rev.*, 1991, **30**, 1675.
2 B. T. Holland, L. Abrams and A. Stein, *J. Am. Chem. Soc.*, 1999, **121**, 4308.
3 C. J. H. Jacobsen, C. Madsen, J. Houzvicka, I. Schmidt and A. Carlsson, *J. Am. Chem. Soc.*, 2000, **122**, 7116.
4 I. Schmidt, A. Boisen, E. Gustavsson, K. Stahl, S. Pehrson, S. Dahl, A. Carlsson and C. J. H. Jacobsen, *Chem. Mater.*, 2001, **13**, 4416.
5 L. M. Huang, Z. B. Wang, J. Y. Sun, L. Miao, Q. Z. Li, Y. S. Yan and D. Y. Zhao, *J. Am. Chem. Soc.*, 2000, **122**, 3530.
6 Y. J. Wang, Y. Tang, Z. Ni, W. M. Hua, W. L. Yang, X. D. Wang, W. C. Tao and Z. Gao, *Chem. Lett.*, 2000, 510.
7 K. H. Rhodes, S. A. Davis, F. Caruso, B. Zhang and S. Mann, *Chem. Mater.*, 2000, **12**, 2832.
8 X. D. Wang, W. L. Yang, Y. Tang, Y. J. Wang, S. K. Fu and Z. Gao, *Chem. Commun.*, 2000, 2161.
9 C. Ke, W. L. Yang, Z. Ni, Y. J. Wang, Y. Tang, Y. Gu and Z. Gao, *Chem. Commun.*, 2001, 783.
10 B. J. Zhang, S. A. Davis, N. H. Mendelson and S. Mann, *Chem. Commun.*, 2000, 781.
11 V. Valtchev and S. Mintova, *Microporous Mesoporous Mater.*, 2001, **43**, 41.
12 V. Valtchev, B. J. Schoeman, J. Hedlund, S. Mintova and J. Sterte, *Zeolites*, 1996, **17**, 408.
13 Y. J. Wang, Y. Tang, X. D. Wang, W. L. Yang and Z. Gao, *Chem. Lett.*, 2000, 1344.
14 Y. Tang, Y. J. Wang, X. D. Wang, W. L. Yang and Z. Gao, *Stud. Surf. Sci. Catal.*, 2001, **135**, 296.
15 M. W. Anderson, S. M. Holmes, N. Hanif and C. S. Cundy, *Angew. Chem., Int. Ed.*, 2000, **39**, 2707.
16 S. M. Holmes, R. J. Plaisted, P. Crow, P. Foran, C. S. Cundy and M. W. Anderson, *Stud. Surf. Sci. Catal.*, 2001, **135**, 296.
17 Y. J. Wang, Y. Tang, X. D. Wang, A. G. Dong, W. Shan and Z. Gao, *Chem. Lett.*, 2001, 1118.
18 W. Xu, J. Dong, J. Li, W. Li and F. Wu, *J. Chem. Soc., Chem. Commun.*, 1990, 755.
19 M. H. Kim, H. X. Li and M. E. Davis, *Microporous Mater.*, 1993, **1**, 191.
20 M. Matsukata, M. Ogura, T. Osaki, P. R. Hari Prasad Rao, M. Nomura and E. Kikuchi, *Topics Catal.*, 1999, **9**, 77.
21 A. E. Persson, B. J. Schoeman, J. Sterte and J.-E. Otterstedt, *Zeolites*, 1994, **14**, 557.
22 M. A. Camblor, A. Corma, A. Mifsud, J. Pérez-Pariente and S. Valencia, *Stud. Surf. Sci. Catal.*, 1997, **105**, 341.
23 G. Decher, *Science*, 1997, **277**, 1232.
24 F. Caruso, R. A. Caruso and H. Mohwald, *Science*, 1998, **282**, 1111.
25 F. Caruso, *Adv. Mater.*, 2001, **13**, 11.
26 T. Sasaki, Y. Ebina, T. Tanaka, M. Harada, M. Watanabe and G. Decher, *Chem. Mater.*, 2001, **13**, 4661.
27 J. A. Martens and P. A. Jacobs, *Zeolites*, 1986, **6**, 334.
28 P. A. Jacobs, E. G. Derouane and J. Weitkamp, *J. Chem. Soc., Chem. Commun.*, 1981, 591.
29 V. Zholobenko, A. Garforth, F. Bachelin and J. Dwyer, *Stud. Surf. Sci. Catal.*, 1997, **105**, 917.
30 R. Szostak, *Molecular Sieves: Principles of Synthesis and Identification*, Blackie Academic & Professional, London, 1998, p. 302.